PERGAMON

International Journal of Heat and Mass Transfer 41 (1998) 4281–4295

International Journal of HEAT and MASS TRANSFER

Rotation induced stabilization of air convection in a bottom heated diverging cylinder rotating about its own axis

Y. T. Ker, T. F. Lin*

Department of Mechanical Engineering, National Chiao Tung University, Hsinchu, Taiwan, R.O.C.

Received 8 September 1997; in final form 6 March 1998

Abstract

Rotation induced stabilization of air convection in a vertical, diverging cylinder heated from below and rotated steadily about its own axis is studied experimentally. The cylinder has a smaller circular cross section at its bottom end. In the experiments, the transient variations of the air temperature at selected locations are measured to explore the effects of rotation rate and diverging angle on the temporal stability of the flow. Data are collected for the diverging angle varied from 0–30°, imposed temperature difference from 5–15°C and rotation rate up to 346.1 rpm. The measured data show that the ranges of the rotation rate to stabilize the flow are wider for diverging cylinders than those for a right cylinder at $\xi = 0^\circ$. Thus, it is possible to use a crucible with a diverging section to grow large and high quality bulk crystals. A power spectrum density analysis of the data for the unstable flow at high rotation rates indicates that the flow oscillation is mainly time periodic and dominated by a single fundamental frequency. Moreover, the oscillation frequency varies nonmonotonically with the rotation rate. Flow regime maps delineating stable and unstable states are also provided for practical applications.

Nomenclature

D_b, D_t diameters of cylinder bottom and top
f_1 first fundamental frequency
g magnitude of the gravitational acceleration
H height of diverging circular cylinder
PSD power spectrum density
Ra Rayleigh number, $\beta g \Delta T D_b^3/\alpha v$
Ra_Ω rotational Rayleigh number, $\beta \Omega^2 \Delta T D_b^4/v\alpha$
t time
T local temperature
Ta Taylor number, $\Omega^2 D_b^4/v^2$
T_H temperature of the hot wall
T_L temperature of the cold wall
R, Φ, Z dimensionless cylindrical coordinate systems scaled with D_b.

Greek symbols
α thermal diffusivity
β thermal expansion coefficient
ΔT temperature difference between the hot and cold walls $T_H - T_L$
Θ dimensionless temperature, $(T-T_L)/(T_H-T_L)$
Θ_{av} nondimensional time-averaged temperature
v kinematic viscosity
τ dimensionless time, $t/D_b^2/\alpha)$
Ω magnitude of rotating rate
ξ diverging angle between insulated wall and gravity (rotating axis).

1. Introduction

Recent interest in the study of thermal convection in a vertical circular cylinder heated from below has been motivated by the important role it plays in growing bulk crystals from solidifying liquid melts. Growth of high quality bulk crystals is relatively important in various microelectronic applications. But unstable melt flow and the associated temperature fluctuation driven by a high thermal buoyancy are known to produce striations in the grown crystals. Microelectronic circuits fabricated on substrates sliced from such defected crystals suffer from reliability problems. Moreover, the melt flow is more

* Corresponding author.

0017–9310/98 $19.00
PII: S0017–9310(98)00104–5

unstable when larger crystals suffer from reliability problems. This is due to the simple fact that the thermal buoyancy in a cylindrical melt-filled crucible is directly proportional to the third power of the crystal diameter D^3 or approximately the melt volume. One effective and simple technique often used to stabilize the thermal buoyancy driven flow is to use crucible rotation. This technique, however, fails to regularize the flow when the thermal buoyancy exceeds a certain critical value. This situation is encountered mainly in growing large crystals. It is speculated that a crucible with a larger cross section in one end near the melt-crystal interface and a smaller cross section in the other end is expected to allow a larger high quality crystal to be grown since the associated buoyancy is substantially below that in a larger non-diverging crucible. In an initial attempt to assess the feasibility of using diverging crucibles experimental measurements were carried out here to investigate effects of crucible rotation on stability of thermal buoyancy driven air flow in a bottom heated trapezoidal cylinder with a diverging cross section in the vertically upward direction. More specifically, time variations of air temperature at selected locations were measured for various imposed temperature differences and rotation rates in three cylinders with the same diameter in their bottoms, $D_b = 5$ cm, but with three different diverging angles.

Considerable attention has been paid in the literature to convection in a bottom heated vertical closed circular cylinder rotating about its axis. Experiments for silicone oil carried out by Hudson and his coworkers [1, 2] indicated that the Nusselt number increases with rotation rate. Steady axisymmetric numerical simulations were carried out by Chew [3]. The onset of steady natural convection was shown by Buell and Catton [4] to be rather sensitive to the lateral thermal boundary condition. Pfotenhauer et al. [5] reported experimental results for the effects of the cylinder geometry and rotation on the onset of convection for low temperature liquid helium. Both the Rayleigh number associated with the convective onset and the heat transfer were found to depend on the rotation rate and aspect ratio of the cell. For water subject to a Rayleigh number in the range $10^6 < Ra < 2 \times 10^{11}$ and Taylor numbers from 10^6 to 10^{12}, Boubnov and Golitsyn [6] experimentally observed a ring pattern of convective flow resulting from the fluid spin-up and vortex interactions between two adjacent vortices. Kirdyashkin and Distanov [7] found that a periodically changing rotation speed can result in periodical temperature changes throughout the entire liquid layer. Asymmetric convection in a vertical cylinder was found to result from lack of the azimuthal symmetry in the imposed wall temperature by Pulicani et al. [8]. Use of appropriate temperature gradients was experimentally demonstrated to produce a flat interface in the vertical Bridgman growth by Feigelson and Route [9]. Control of the furnace temperature profile near a melt–solid interface was noted to be most effective in producing a flat interface [10]. Convection is produced relative to the solid-body rotation through the coupling of the centrifugal acceleration and density variations in the fluid. A mathematical analysis of the centrifugally driven thermal convection in a cylinder rotating about its own vertical axis was carried out by Homsy and Hudson [11].

Visualization of a flow of silicone oil with $Pr = 10^5$ in a stationary, vertical cylinder heated from below revealed axisymmetric flow at slightly supercritical Rayleigh number and two distinct three-dimensional flow motions at increasing Rayleigh numbers [12]. Various routes for transition from steady laminar flow to unsteady chaotic flow were experimentally determined by Rosenberger and his colleagues [13, 14] for Xenon gas in a bottom heated vertical cylinder. Both the Rule-Takens and period-doubling routes were reported for different ranges of the Rayleigh number. Similar experimental study was conducted by Kamotani et al. [15] for gallium melt ($Pr = 0.027$) for both vertical and inclined cylinders. Based on the temperature data, various convection flow patterns were inferred.

Another geometry of considerable interest is convection in a bottom heated, infinitely bounded horizontal layer of fluid rotating at a constant angular speed about a vertical axis [16–22]. From a linear stability analysis, Niller and Bisshopp [16] noted that in the limit of large Taylor number the viscous effects play an important role in a thin layer near the boundary and the critical Rayleigh number Ra_c for the onset of convection is independent of whether the boundaries are rigid or free. A numerical analysis conducted by Veronis [17] indicated that the Prandtl number exhibits significant effects on the flow and thermal structures. For the limit of infinite Prandtl number Küpper and Lortz [18] showed that no stable steady-state convective flow exists if the Taylor number exceeds a certain critical value. Rossby [19] experimentally observed the subcritical instability in a water layer for $Ta > 5 \times 10^4$ and in a mercury layer for $Ta < 10^5$. In addition, for water at $Ra > 10^4$ the Nusselt number was found to increase with the Taylor number. The opposite trend holds for mercury. Besides, at large Taylor number oscillatory convection is preferred in mercury. Based on the mean-field approximation, Hunter and Riahi [20] analytically showed the nonmonotonic variation of the Nusselt number with the Taylor number. The linear stability analysis from Rudraiah and Chandna [21] indicated that the critical Rayleigh number was relatively sensitive to the method and rate of heating, Coriolis force and the nature of the bounding surfaces of the fluid layer. The analysis from Clever and Busse [22] suggests that the critical Rayleigh number for the onset of oscillatory motion increases with the Taylor and Prandtl numbers.

Experimental data for the Nusselt number in a top heated horizontal rectangular cavity of silicone oil ro-

tating about a vertical axis passing through the geometric center of the cavity were presented by Abell and Hudson [23]. Hathaway and Somerville [24] conducted a numerical simulation of an inclined rotating layer with the rotation vector tilted from the vertical. The tilting of the rotation vector was found to produce significant change in the flow structure. A combined theoretical, numerical and experimental study was presented by Bühler and Oertel [25] to investigate thermal convection in a rotating rectangular shallow box heated from below. First, a linear stability analysis was used to predict the onset of steady and oscillatory convection and three-dimensional flow configuration. Then, a numerical analysis predicted the change of the roll orientation with the Taylor number. Finally, flow structures at various Rayleigh and Taylor numbers were visualized. Unusual flow circulation was experimentally observed by Condie and Griffiths [26] for a horizontal layer of water.

The above literature review indicates that previous studies mainly focused on the effects of rotation on the onset of convection and the overall heat transfer at supercritical Rayleigh numbers. The processes on how rotation affects the flow stability and unsteady thermal characteristics are not well understood. Moreover, no study has been reported for the thermal buoyancy driven flow characteristics in a rotating diverging cylinder. To investigate the possibility of using trapezoidal crucibles to grow large crystals, an experimental study was carried out here to explore rotation induced flow stabilization in a thermal buoyancy driven air flow in a bottom heated diverging cylinder with a larger top end.

2. Experimental apparatus

The experimental system established for measuring the thermal characteristics in convection of air in the rotating vertical diverging circular cylinders, schematically shown in Fig. 1, consists of four parts—rotating frame, test section, temperature control unit and temperature measuring unit. Fig. 2 shows the details of the test section in the rotating assembly. Specifically, the trapezoidal cavity of air is rotated at a constant angular speed Ω about its own axis.

The rotating frame is made up of a rotary table of 31.5 cm in diameter and is mounted on a steel shaft of 3 cm in diameter. The frame is designed to provide a space of 27.6 cm in diameter and 27.3 cm in height for housing the test section. The shaft is rotated by a 2 horse-power d.c. motor with its speed controlled by an inverter. In addition, the rotating speed is detected by a photoelectric tachometer. Care is taken to ensure the table to rotate centrally and steadily so that the accuracy of the rotation rate is within 0.3%.

The test section fixed on the rotating table is an air-containing diverging circular cylinder of 10 cm in height and 5 cm in bottom diameter (Fig. 2). The diameter of the cylinder top is chosen to be at 5 cm, 7.5 cm or 10 cm with the corresponding diverging angle $\xi = 0^\circ$, 15° or 30° (Fig. 3). The top and bottom of the cylinder are both made of two 2 mm thick copper plates with 8 mm thick OMEGABOND OB-101 epoxy sandwiched between them (Fig. 3) and are controlled at uniform but different temperatures by circulating constant temperature coolants through them. Two fluid sliprings are used to allow the coolants to pass from stationary thermostats to the rotating cavity. The thermostats used are the LAUDA RK-20 compact constant temperature baths with a temperature range of -40–150°C and a resolution of 0.1°C. Care must be taken to prevent coolant leak from the fluid sliprings. The side wall of the cylinder is made of 5 mm thick acrylic plates and is thermally insulated by superlon foam. Through this arrangement the temperature uniformity of the isothermal plates can be controlled to within $\pm 0.1^\circ$C. The sampled measured data for the temperature of the hot bottom and cold top walls at selected locations are given in Table 1.

For temperature measurement, thermocouple connections are carefully arranged in the rotating cylinder. In particular, seven T-type thermocouples are fixed at the designated locations (Fig. 3) by high performance fine Neoflon threads, which are in turn fixed on the side wall of the cylinder and pass through the axis of the cylinder. Prior to installation the thermocouples were calibrated by the LAUDA thermostats and high precision liquid-in-glass thermometers. The voltage signals from the thermocouples were passed through a slip ring to the HP 3852A data acquisition/control system with a personal computer for further data processing. Data collection is normally started when the flow already reaches a steady or statistically stable state. In view of the low speed flow encountered in the rotating cavity, velocity measurement is difficult and is not conducted here.

The test was started by first setting the thermostats at the predetermined temperatures and then recirculating the coolants through the top and bottom of the rotating cylinder. The mean value of the hot and cold plate temperatures is adjusted to be approximately equal to the ambient temperature, so that heat loss from the cavity to the ambient can be reduced and thermal radiation across the plates is minimized. In the meantime the cavity was rotated at a predetermined speed. Then the temperature of the air inside the cavity was measured at selected locations. After the transient stage has elapsed, data for the steady or statistically stable state were stored and analyzed. The repeatability of the experimental data was good when the initial condition of the test was controlled at the same state.

The ranges of the governing parameters to be investigated are as follows: the rotating speed varied from 0–346.1 rpm and the temperature difference across the cavity from 5–15°C for the three vertical diverging cylinders.

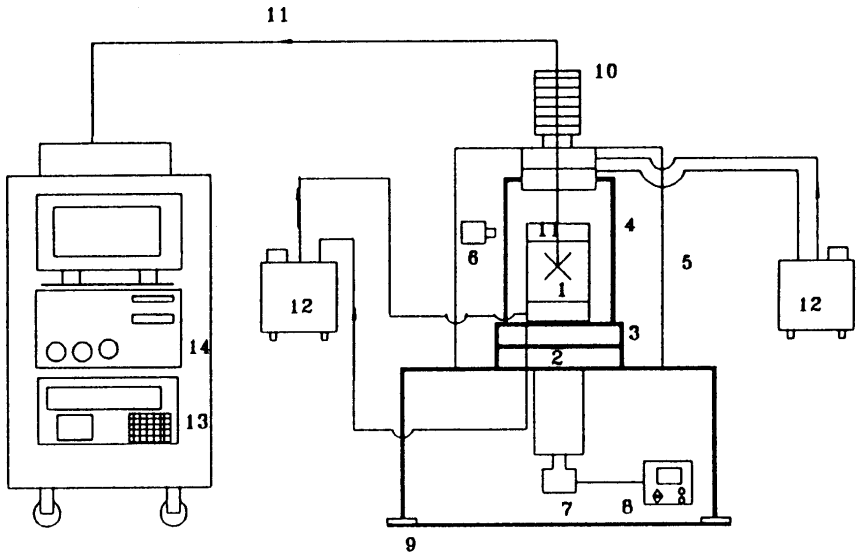

1 : test section
2 : fluid slip ring
3 : supporting frame
4 : rotating frame
5 : statatic frame
6 : photo – electric tachometer
7 : 2 Hp induction motor
8 : inverter
9 : platform
10 : slip ring
11 : thermocouples
12 : thermostat
13 : data acquisition system
14 : P.C. computer

Fig. 1. Schematic diagram of the experimental system.

The results from uncertainty analysis of the measurement are summarized in Table 2.

3. Results and discussion

In the following only a small sample of the long term results for the time variations of the air temperature at selected locations at statistically steady state from the present measurements will be presented to illustrate flow stabilization by the axial cavity rotation in the diverging cylindrical air enclosure at various rotation rates and subject to various temperature differences across its top and bottom. Attention will also be paid to the effects of the diverging angle on the rotation induced flow stabilization. The requirements which are applied to obtain steady or statistically stable state conditions are as follows. First, the experiment is operated for at least 50 times of the thermal diffusion time D_b^2/α, which is about 3 h. Then, we insure that the change in the time-average temperature measured from each thermocouple is less than $\pm 0.1^\circ$C for a period of at least 15 min. Note that in presenting the following results the bottom diameter of the cylinder is chosen to be the characteristic length.

The spatial dependence of the temperature oscillation is examined first. Typical data to show this dependence are given in Fig. 4 for two cases in which the time records of air temperature at various locations for $\Omega = 169.1$ rpm and $\Delta T = 5^\circ$C and 15°C at the diverging angle $\xi = 30^\circ$ are displayed. Since only the data at steady or statistically steady state are recorded, the time instant $\tau = 0$ denotes a certain arbitrary instant in that state. The results clearly indicate that the air temperature oscillates at nearly the same frequency at various locations for a given set of Ω, ΔT and ξ. But the oscillation amplitude shows some space dependence. Specifically, a slightly stronger oscillation is noted at the three locations along the cylinder axis in the top half of the cylinder for $Z \geqq 0$. Off the axis oscillation is slightly weaker. This trend in the space dependence of the flow oscillation is noted for all cases investigated here.

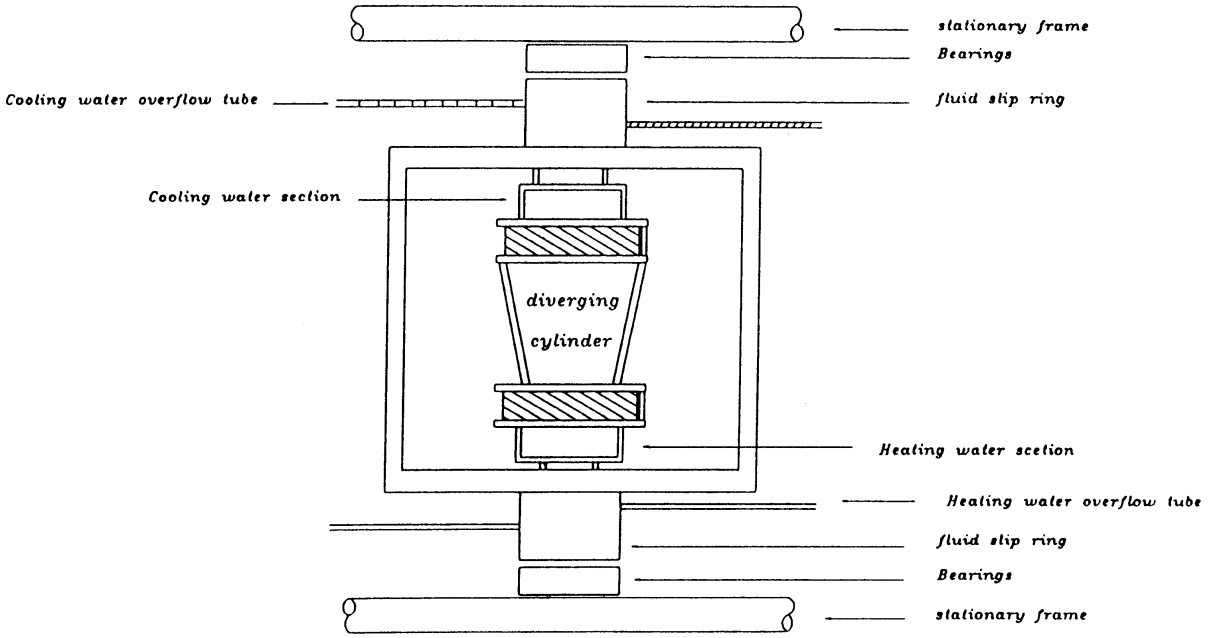

Fig. 2. Rotating assembly for vertical diverging cylinder.

Next, effects of the diverging angle on the rotating flow stability are revealed by inspecting the measured time histories for various Ω, ΔT and ξ. Figures 5 (a)–(c) compares the present data at a representative location selected at the origin of the coordinates for $\Delta T = 5\ ^{\circ}\mathrm{C}$ for Ω up to 346.1 rpm at $\xi = 0^{\circ}$, 15° and 30°. The results in Fig. 5 (a) for the vertical right cylinder at $\xi = 0^{\circ}$ indicate that at this low ΔT the thermal buoyancy driven flow in a stationary cavity ($\Omega = 0$ is steady at long time after some transient oscillation has passed. As the cylinder rotates slowly at 30.8 rpm, a large amplitude time periodic oscillation is induced. It is of interest to note that at a slightly higher rotation rate of 43.5 rpm the amplitude of the temperature oscillation is less than 0.014 dimensionlessly or 0.07°C. In fact, this small amplitude oscillation can be considered as resulting from the background disturbances which always exist in the test apparatus ad the flow is essentially steady. In the range of Ω from 43.5–140.2 rpm, the oscillation amplitude is all below 0.13°C and the flow can be regarded as steady. As Ω is raised to 169.1 rpm and over, the temperature oscillation grows slightly with the rotation rate. The flow is time periodic or quasi-periodic depending on the rotation rate. Moreover, substantial change in the oscillation frequency with the rotation rate exists. The characteristics of the oscillation frequency will be discussed later when the results from the power spectrum analysis of the data are presented. In the diverging cylinder with $\xi = 15^{\circ}$, more space is provided for the thermal buoyancy driven air flow to move and the flow is already in a large amplitude oscillation with time when the cylinder is non-rotating ($\Omega = 0$), as evident from the data in Fig. 5(b). But rotating the cylinder at a rate ranging from 30.8–140.2 rpm stabilizes the flow with all the oscillation amplitudes being below 0.18°C. For $\Omega \geqq 169.1$ rpm, the flow again oscillates noticeably with time and the oscillation amplitude increases slightly with the rotation rate. Similar characteristics in the rotation induced flow stabilization are noted for a larger diverging angle of 30° (Fig. 5(c)). The above results for $\Delta T = 5^{\circ}\mathrm{C}$ and three diverging angles clearly show that the range of the rotation rate in which the flow is stabilized by the cavity rotation is not reduced by increasing the diverging angle.

To further illustrate the effects of the diverging angle on the rotation induced flow stabilization, results for higher thermal buoyancies at $\Delta T = 10^{\circ}\mathrm{C}$ and 15°C are examined in the following. The results given in Figs 6(a)–(c) for $\Delta T = 10^{\circ}\mathrm{C}$ suggest that at this higher thermal buoyancy the flow is in a large amplitude, irregular oscillation for $\xi = 0^{\circ}$, 15° and 30° when the cylinder is stationary ($\Omega = 0$). At $\xi = 0^{\circ}$ rotating the cylinder slowly at 30.8 and 43.5 rpm causes the flow to oscillate time periodically (Fig. 6(a)). But the oscillation amplitude is still large. As the rotation rate is raised further with Ω between 59.8 and 140.2 rpm, the flow oscillation is suppressed substantially. The oscillation amplitude is smaller than 0.17°C and the flow is regarded as steady. For $\Omega \geqq 169.1$ rpm, the cavity rotation does not stabilize the flow. The results in Fig. 6(b) for the diverging cylinder with $\xi = 15^{\circ}$ show that at $\Omega = 0$ the flow is also in a large amplitude,

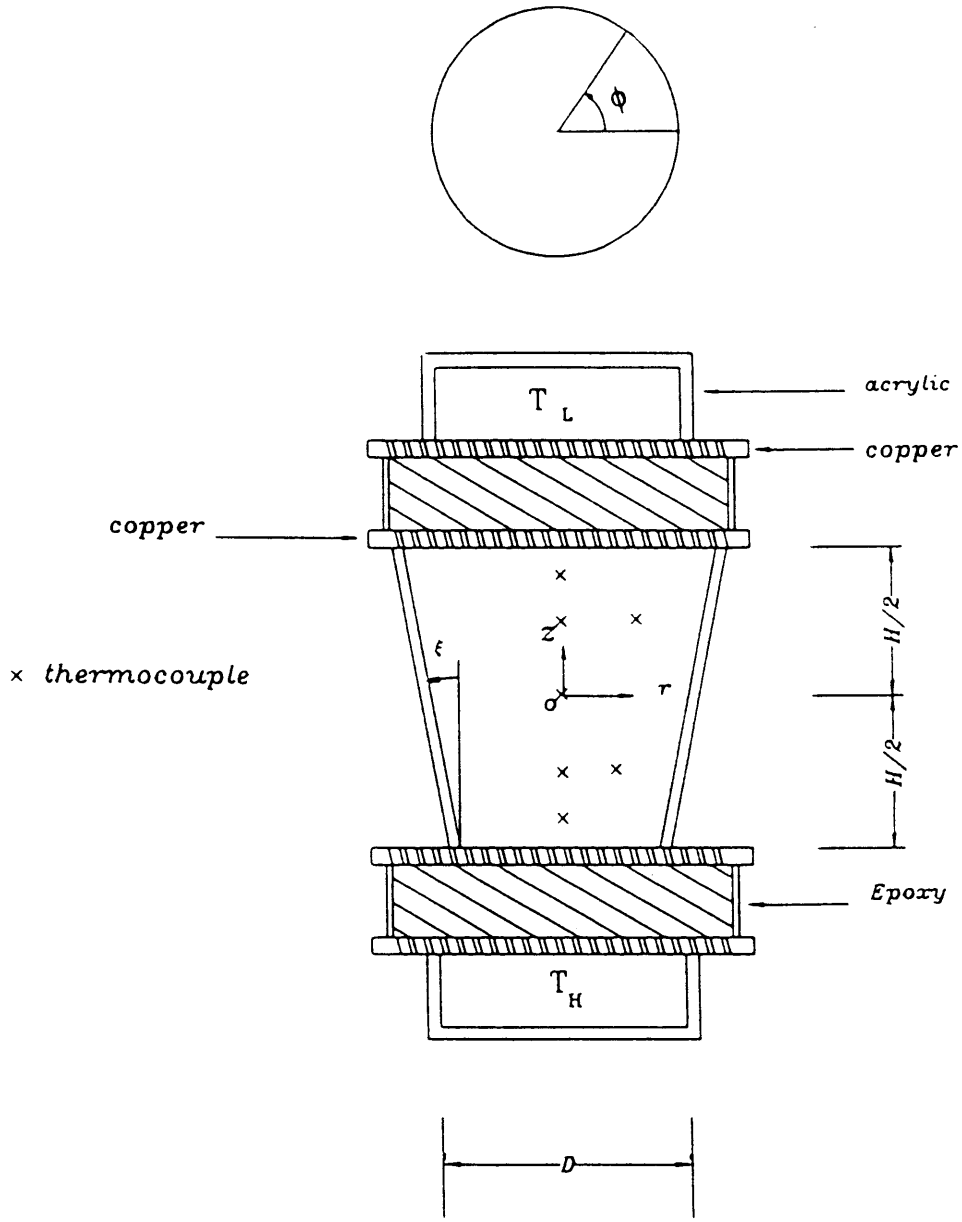

Fig. 3. Test section assembly for diverging cylinder.

random oscillation as that in a right cylinder with ($\xi = 0^\circ$) discussed above. When the rotation rate ranges from 30.8–198.3 rpm, the oscillation amplitudes are all below 0.2°C, suggesting the flow being essentially steady. Note that this range of the rotation rate for the flow to be stabilized is wider for $\xi = 15^\circ$ than that for $\xi = 0^\circ$. For $\Omega \geqq 227.7$ rpm, the flow oscillates noticeably. In the cylinder with a larger diverging angle of 30°, Fig. 6(c) shows that the flow is an intensive irregular oscillation at $\Omega = 0$ and 30.8 rpm. For Ω ranging from 43.5–140.2 rpm, the cavity rotation greatly suppresses the flow oscillation so that its amplitude all below 0.2°C and steady flow results. It is important to note that the range of the rotation rate for the steady flow to exist is slightly wider for $\xi = 30^\circ$ than that for $\xi = 0^\circ$. Similar conclusions can be draw from the results for a high thermal buoyancy for $\Delta T = 15$°C. In summary, these results clearly suggest that cavity rotation can still effectively stabilize the flow in a sufficiently wide range of the rotation rate in the diverging cylinders studied here.

Table 1
Temperature uniformity in isothermal walls for $\Omega = 0$ of diverging cylinder at $\xi = 30^\circ$

Location (R, Φ)	T_L (°C)	Location (R, Φ)	T_H (°C)
0.4, 0.0	14.90	0.4, 0.0	35.07
0.4, 0.5π	14.86	0.4, 0.5π	35.01
0.4, π	14.93	0.4, π	35.04
0.4, 1.5π	14.97	0.4, 1.5π	34.99
0.0, 0.0	14.94	0.0, 0.0	35.02
0.25, 0.25π	14.88	0.25, 0.25π	35.05
0.25, 0.75π	14.90	0.25, 0.75π	35.10
0.25, 1.25π	14.97	0.25, 1.25π	35.07
0.25, 1.75π	14.91	0.25, 1.75π	35.02

Table 2
Summary of uncertainty analysis for diverging circular cylinders

Parameters	Uncertainty
D_b, D_t (m)	$\pm$0.00025 m
H (m)	$\pm$0.00025 m
T_H, T_L	$\pm$0.1°C (non-rotating)
T_H, T_L	$\pm$0.2°C (rotating)
T (Thermocouples)	$\pm$0.05°C
α (m^2s^{-1})	$\pm$0.07%
β (K^{-1})	$\pm$0.05%
ρ (Kg m^{-3})	$\pm$0.05%
ν (m^2 s^{-1})	$\pm$0.07%
Ω (rpm)	$\pm$0.3%
ξ (degree)	$\pm$0.25°
Ta	$\pm$10.5%
Ra	$\pm$8.5%
Ra_Ω	$\pm$11.5%

The detailed characteristics of the flow oscillation in the rotating, diverging cylinders are further explored by examining the frequencies of the measured time records of the air temperature evaluated by a fast Fourier Transform analysis. Attention is focused on the change of the oscillation frequency with the rotation rate at different ΔT and ξ for the unstable cases with $\Omega \geqq 169.1$ rpm. An inspection of the results for the power spectrum densities (PSD) given in Fig. 7(a)–(c) for $\Delta T = 5$°C reveals that the temperature oscillations at various Ω and ξ are mainly dominated by different single fundamental frequencies. Second fundamental mode appears in some cases and is very close to the first mode. Thus the flow is time periodic or quasi-periodic. Moreover, for each diverging angle the oscillation frequency varies nonmonotonically with the rotation rate. More specifically, in the right cylinder ($\xi = 0^\circ$) the flow oscillates at a very low frequency of 0.019 Hz for $\Omega = 169.1$ rpm (Fig. 7(a)). A small raise of Ω to 198.3 rpm causes a large increase of the frequency to 0.504 Hz. But the oscillation frequency drops for a further increase in the rotation rate. Note that the frequency rises again when Ω is raised from 257.2 to 286.7 rpm. Beyond that, the frequency also decreases with an increase in Ω. Similar trend can be seen in Fig. 7(b) and (c) for the diverging cylinders with $\xi = 15^\circ$ and 30°. Contrasting the frequency data at the same rotation rate in Fig. 7(a)–(c) shows a significant dependence of the frequency of the diverging angle. This nonmonotonic variation of the frequency with the rotation rate and the dependence of the frequency on the diverging angle can also be seen from the data in Figs 8 and 9 at higher thermal buoyancies with $\Delta T = 10$°C and 15°C. Comparing the corresponding plots at the same Ω in Figs 7–9 for three different ΔT discloses that the oscillation frequency depends only weakly on the imposed temperature difference. It is of interest to note from Fig. 8(b) and (c) that in the diverging cylinders at $\Delta T = 10$°C, the two fundamental frequency modes characterizing quasi-periodic oscillations separate from each other to a certain degree for the rotation rates $\Omega = 227.7$ rpm at $\xi = 15$°C and $\Omega = 257.2$ rpm at $\xi = 30^\circ$.

An overall characteristic of the flow stabilization by the cavity rotation in the diverging cylinders can be conveniently expressed by the time-average energy of the dimensionless air temperature fluctuation $\overline{(\Theta - \Theta_{av})^2}$ where Θ and Θ_{av} are respectively the instantaneous and time-average, measured air temperatures. Typical results for the energy of temperature fluctuation are shown in Fig. 10 for $\Delta T = 5$, 10 and 15°C for $\xi = 0^\circ$ and 30° at the chosen origin of the coordinates for various Ω. The effects of the cavity rotation on the flow stability can be clearly seen from these results. Specifically, in the range of Ω from 45.3–120 rpm, the fluctuation energy is small for $\xi = 0^\circ$, 15° and 30° and the flow oscillation can be effectively suppressed by the axial cylinder rotation.

4. Concluding remarks

Through detailed experimental measurements of time histories of air temperature in a differentially heated diverging air-filled cylinder, the effects of the diverging angle and rotation rate on the temporal stability of the flow were investigated. The experiments were carried out for three different imposed temperature differences at $\Delta T = 5$°C, 10°C and 15°C and rotation rate $\Omega = 0$–346.1 rpm at three diverging angles 0°, 15° and 30°. The measured data show that the ranges of the rotation rate for the flow to be stabilized are wider for diverging cylinders at $\xi = 15^\circ$ and 30° than those for a right cylinder at $\xi = 0^\circ$. These results suggest that a crucible with a diverging section can be used to grow large and high quality bulk crystals. Examining the temporal characteristics of the unstable flow at high rotation rates shows that the

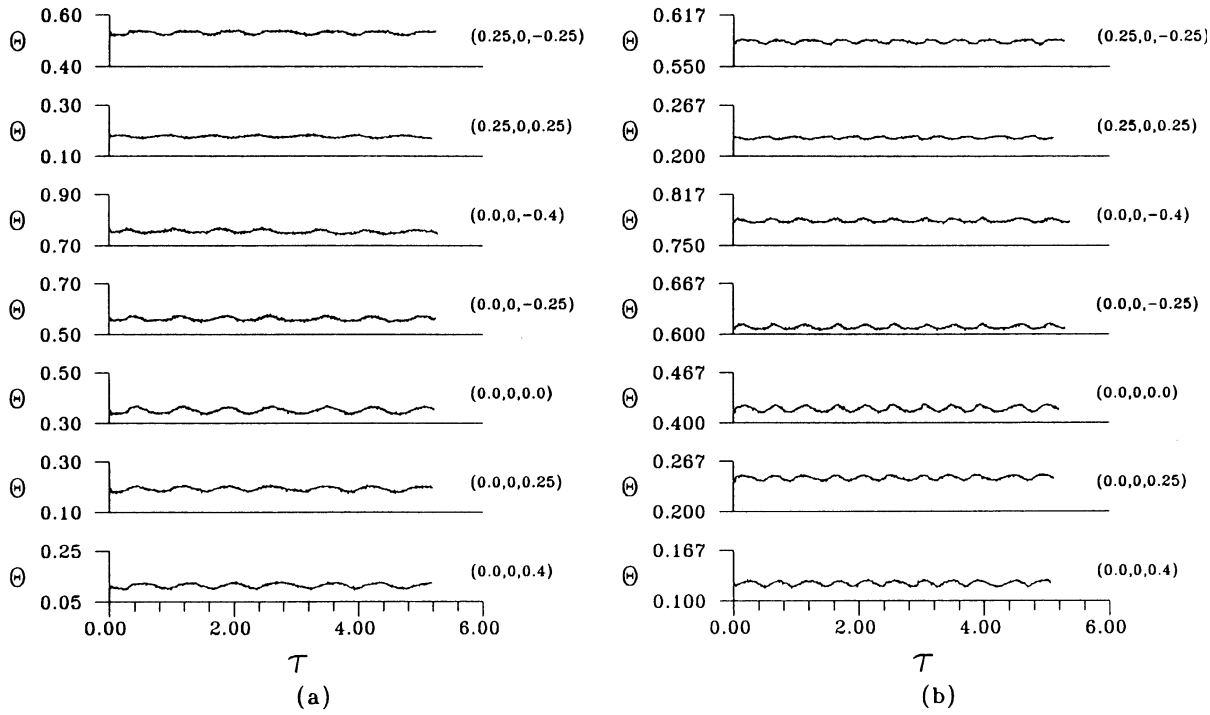

Fig. 4. Measured time histories of the air temperature at various locations and diverging angle $\xi = 30^\circ$ for $\Omega = 169.1$ rpm ($Ta = 8.71 \times 10^6$) for (a) $\Delta T = 5^\circ$C ($Ra = 5.89 \times 10^4$) and (b) $\Delta T = 15^\circ$C ($Ra = 1.77 \times 10^5$).

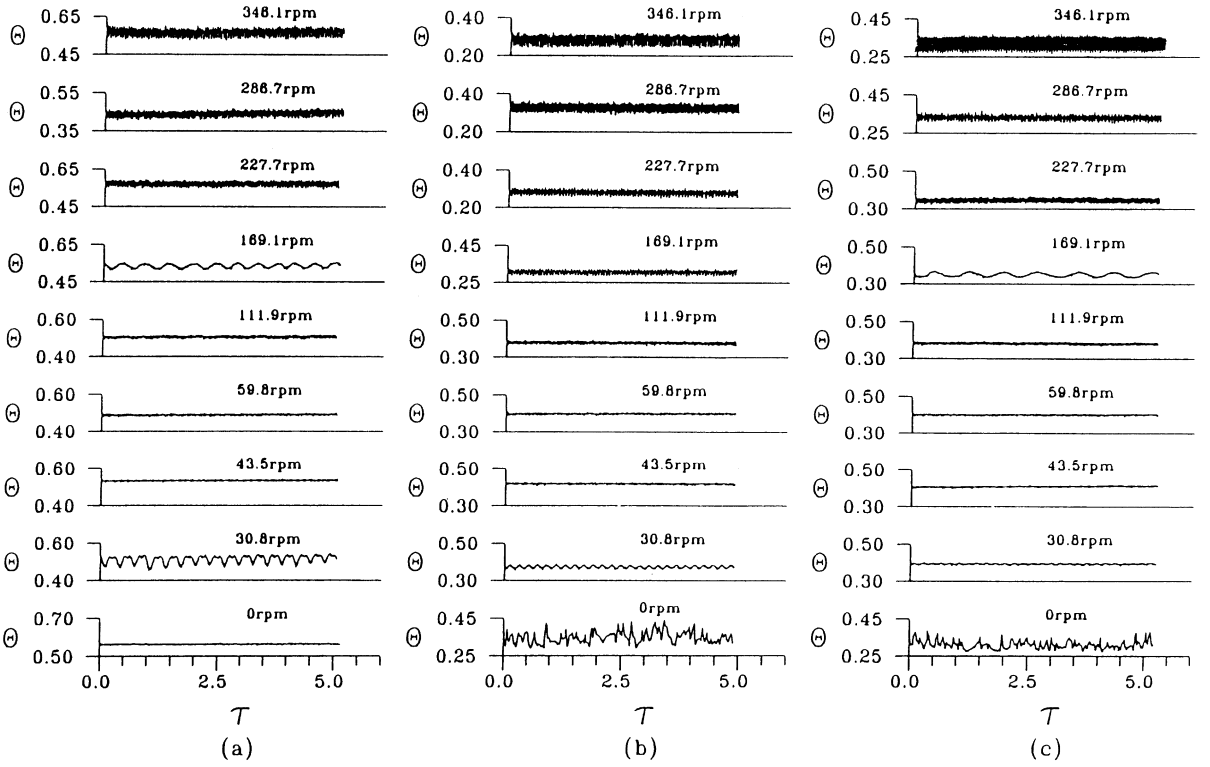

Fig. 5. Measured time records of the air temperature at location $(R, \Phi, Z) = (0,0,0)$ for various rotation rates at $\Delta T = 5^\circ$C ($Ra = 5.89 \times 10^4$) for cylinder with diverging angle (a) $\xi = 0^\circ$, (b) $\xi = 15^\circ$ and (c) $\xi = 30^\circ$.

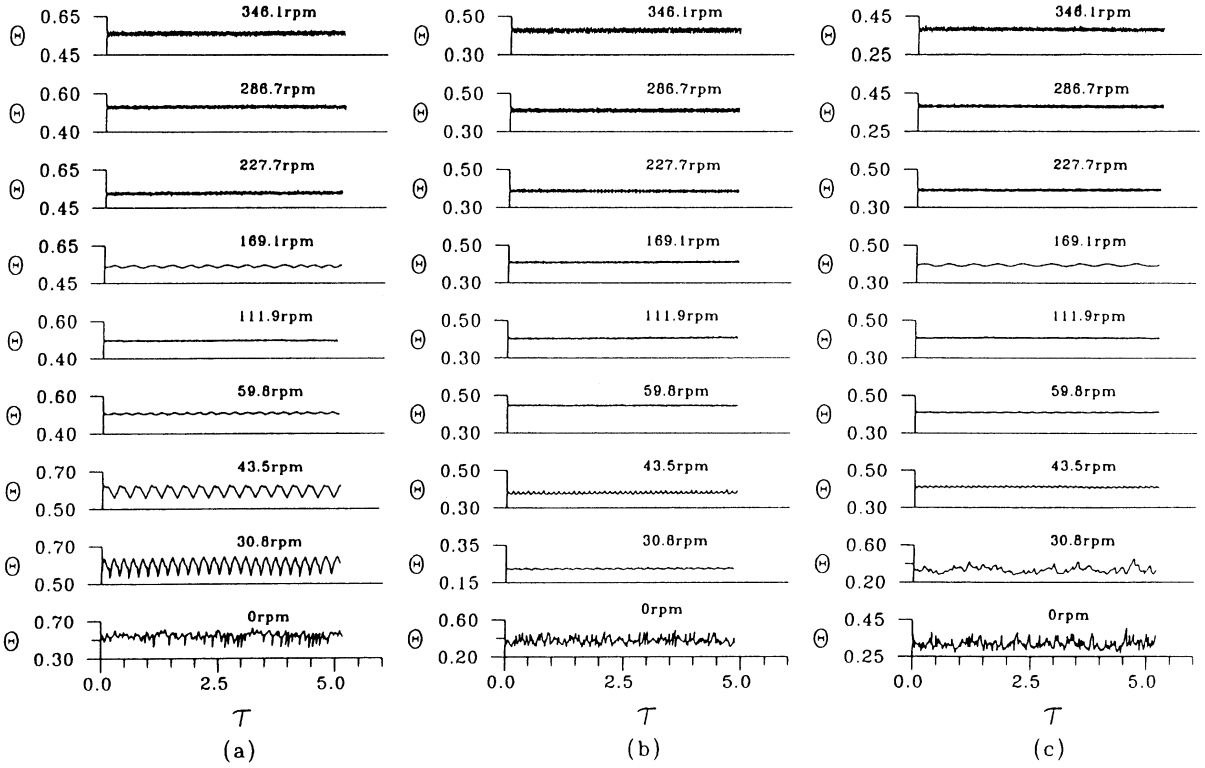

Fig. 6. Measured time records of the air temperature at location $(R, \Phi, Z) = (0,0,0)$ for various rotation rates at $\Delta T = 10°C$ $(Ra = 1.18 \times 10^5)$ for cylinder with diverging angle (a) $\xi = 0°$, (b) $\xi = 15°$ and (c) $\xi = 30°$.

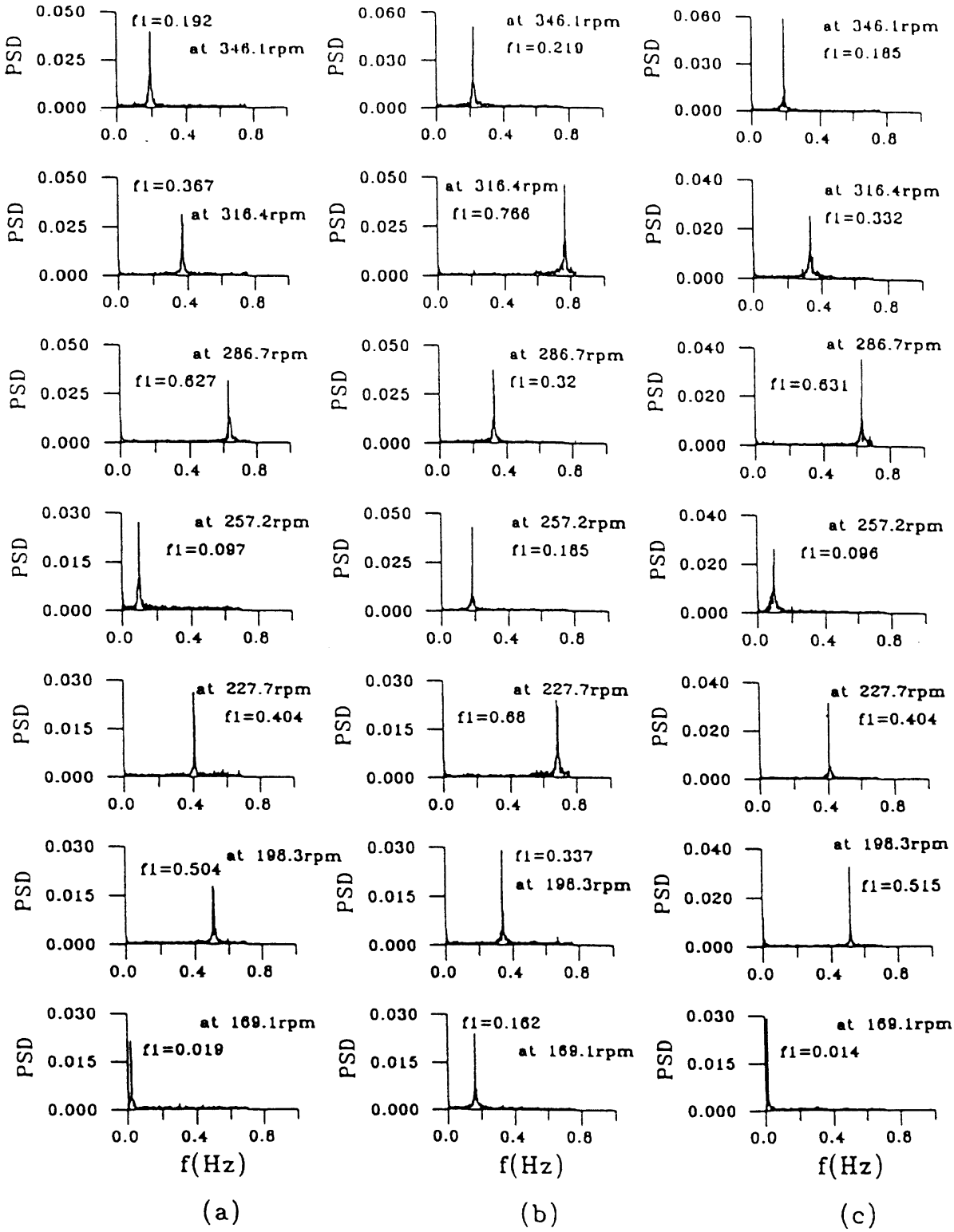

Fig. 7. Power spectrum densities of the air temperature at location $(R, \Phi, Z) = (0,0,0)$ for various rotation rates at $\Delta T = 5°C$ ($Ra = 5.89 \times 10^4$) for cylinder with diverging angle (a) $\xi = 0°$, (b) $\xi = 15°$ and (c) $\xi = 30°$.

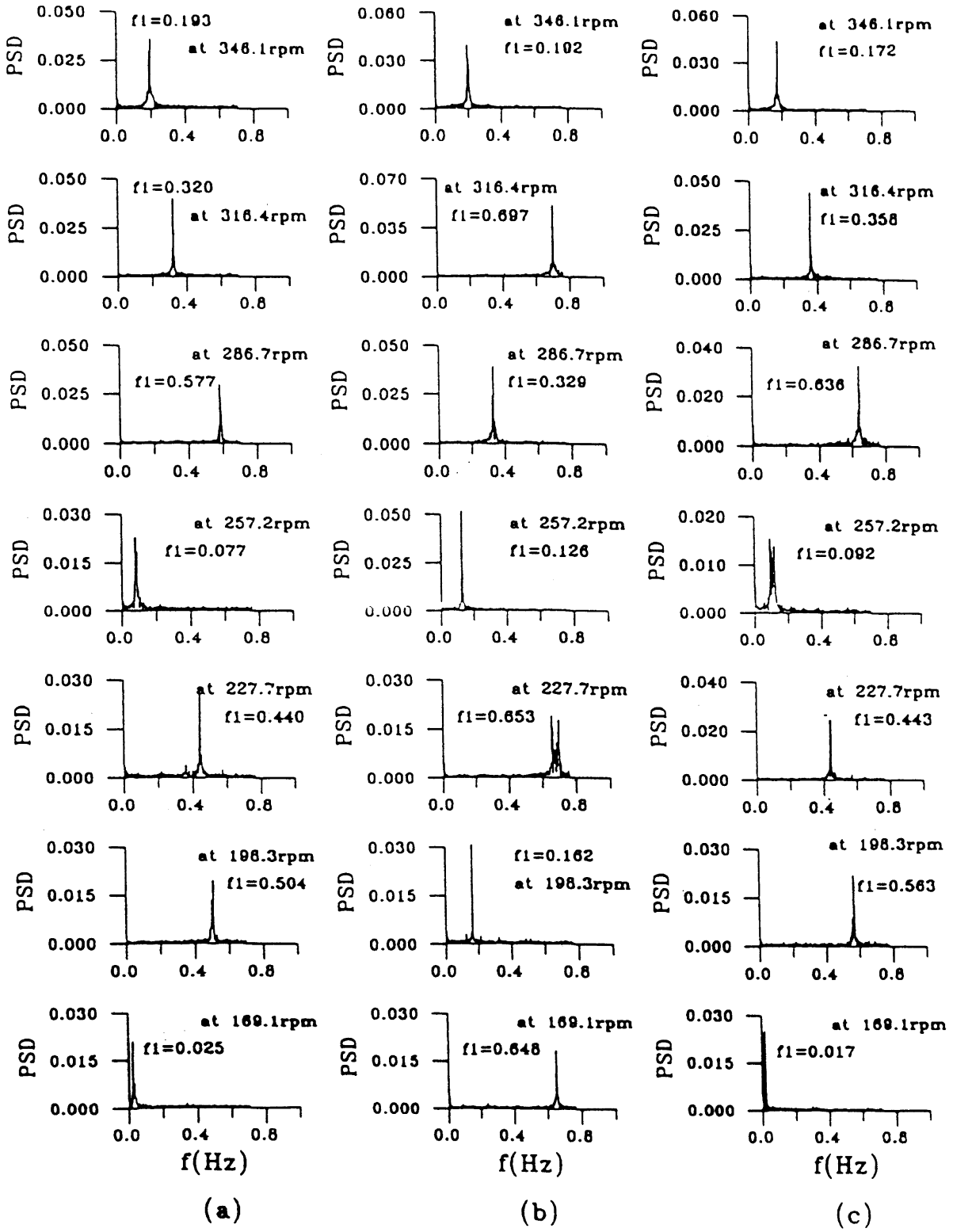

Fig. 8. Power spectrum densities of the air temperature at location $(R, \Phi, Z) = (0,0,0)$ for various rotation rates at $\Delta T = 10°C$ ($Ra = 1.18 \times 10^5$) for cylinder with diverging angle (a) $\xi = 0°$, (b) $\xi = 15°$ and (c) $\xi = 30°$.

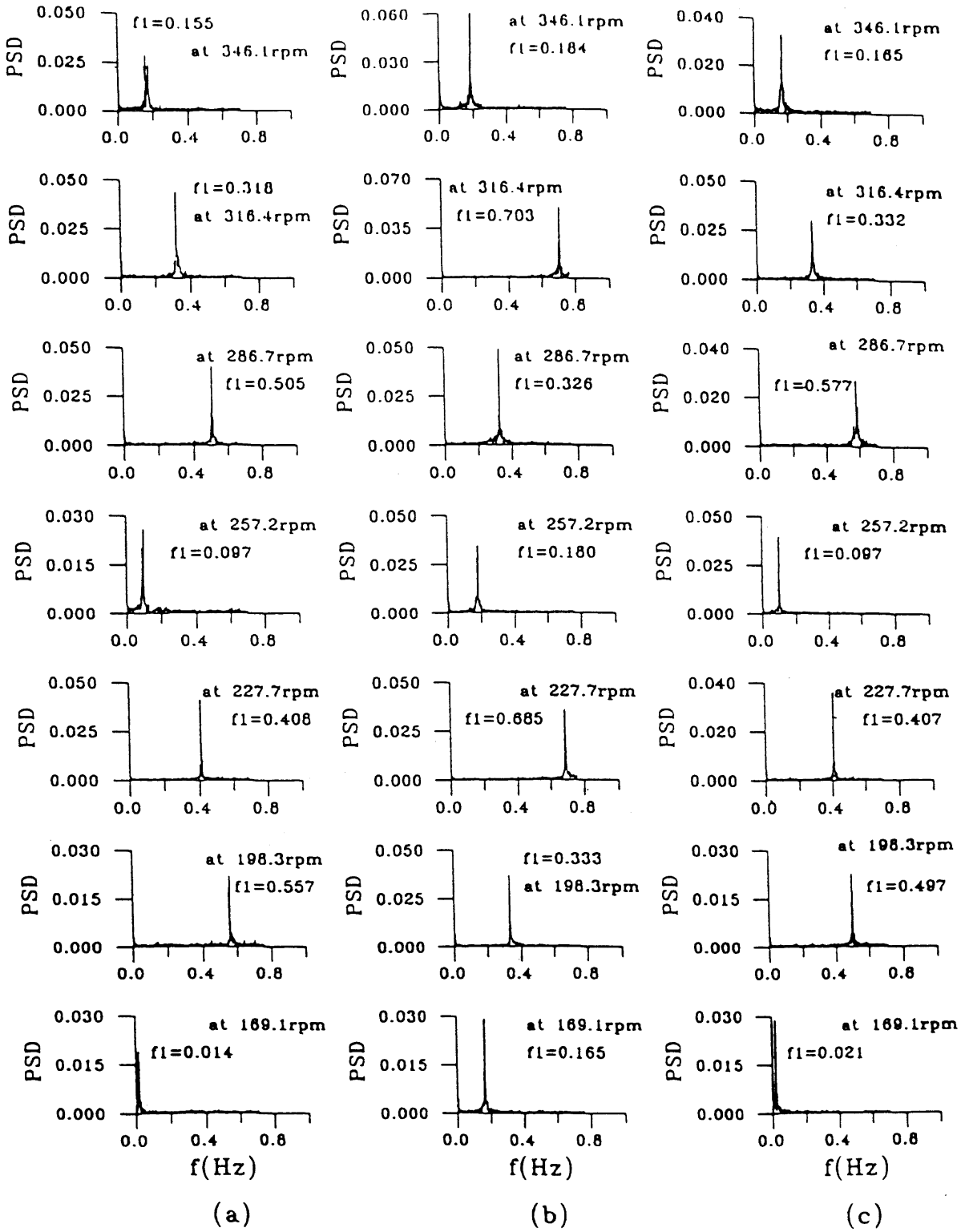

Fig. 9. Power spectrum densities of the air temperature at location $(R, \Phi, Z) = (0,0,0)$ for various rotation rates at $\Delta T = 15°C$ ($Ra = 1.77 \times 10^5$) for cylinder with diverging angle (a) $\xi = 0°$, (b) $\xi = 15°$ and (c) $\xi = 30°$.

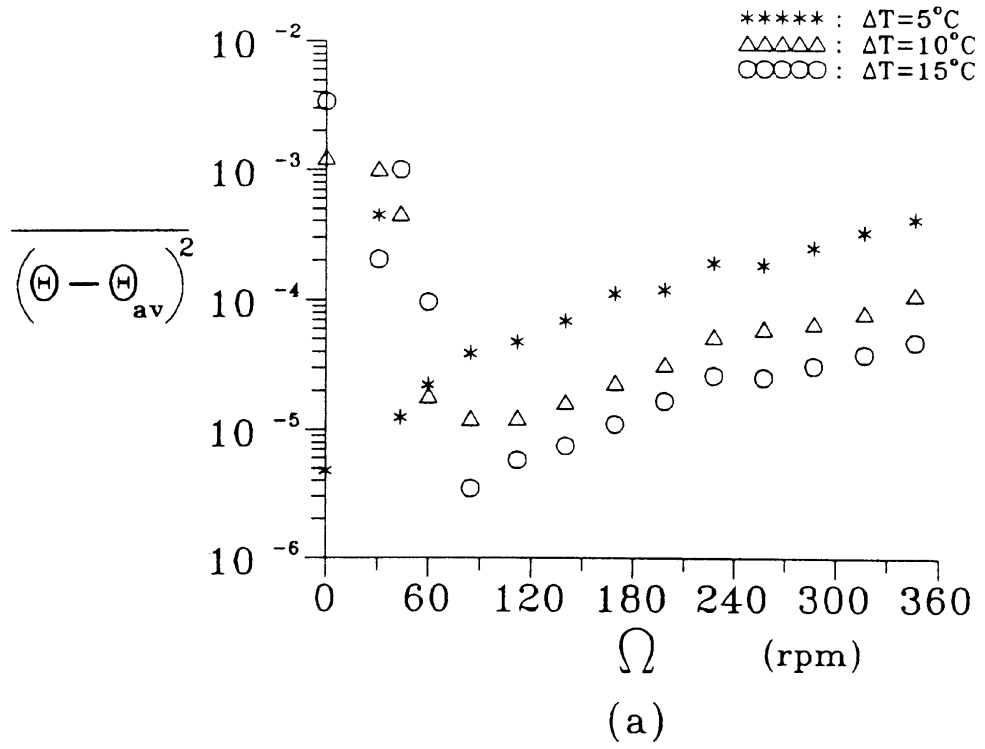

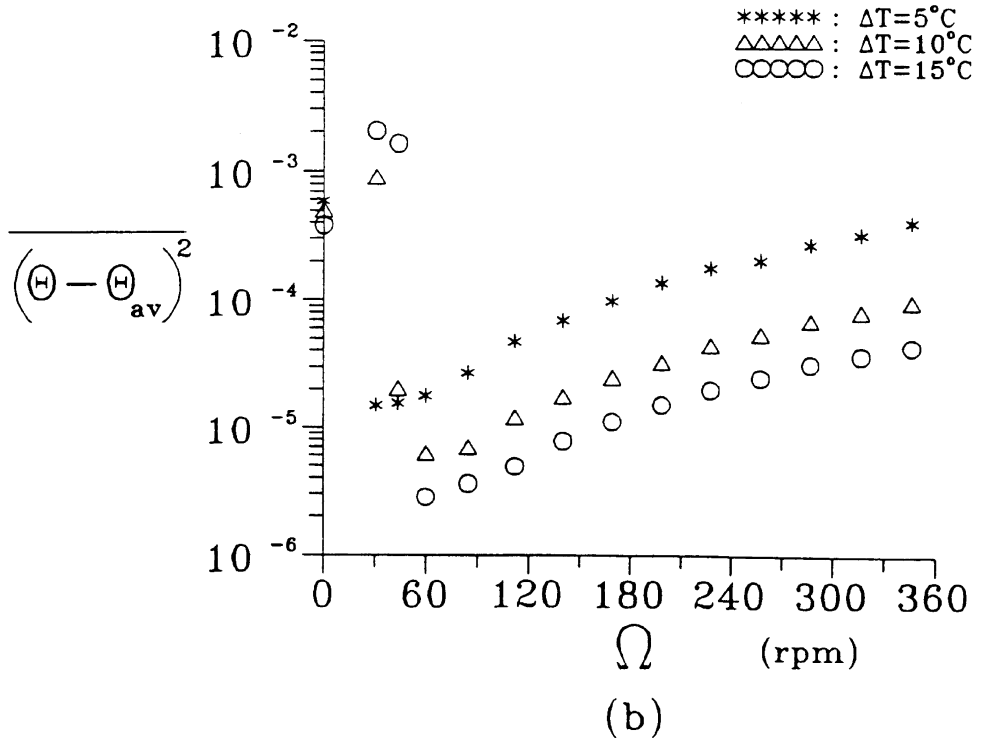

Fig. 10. Variations of time-average energy of temperature fluctuation with rotation rate at different ΔT for cylinders with diverging angle (a) $\xi = 0°C$ and (b) $\xi = 30°$.

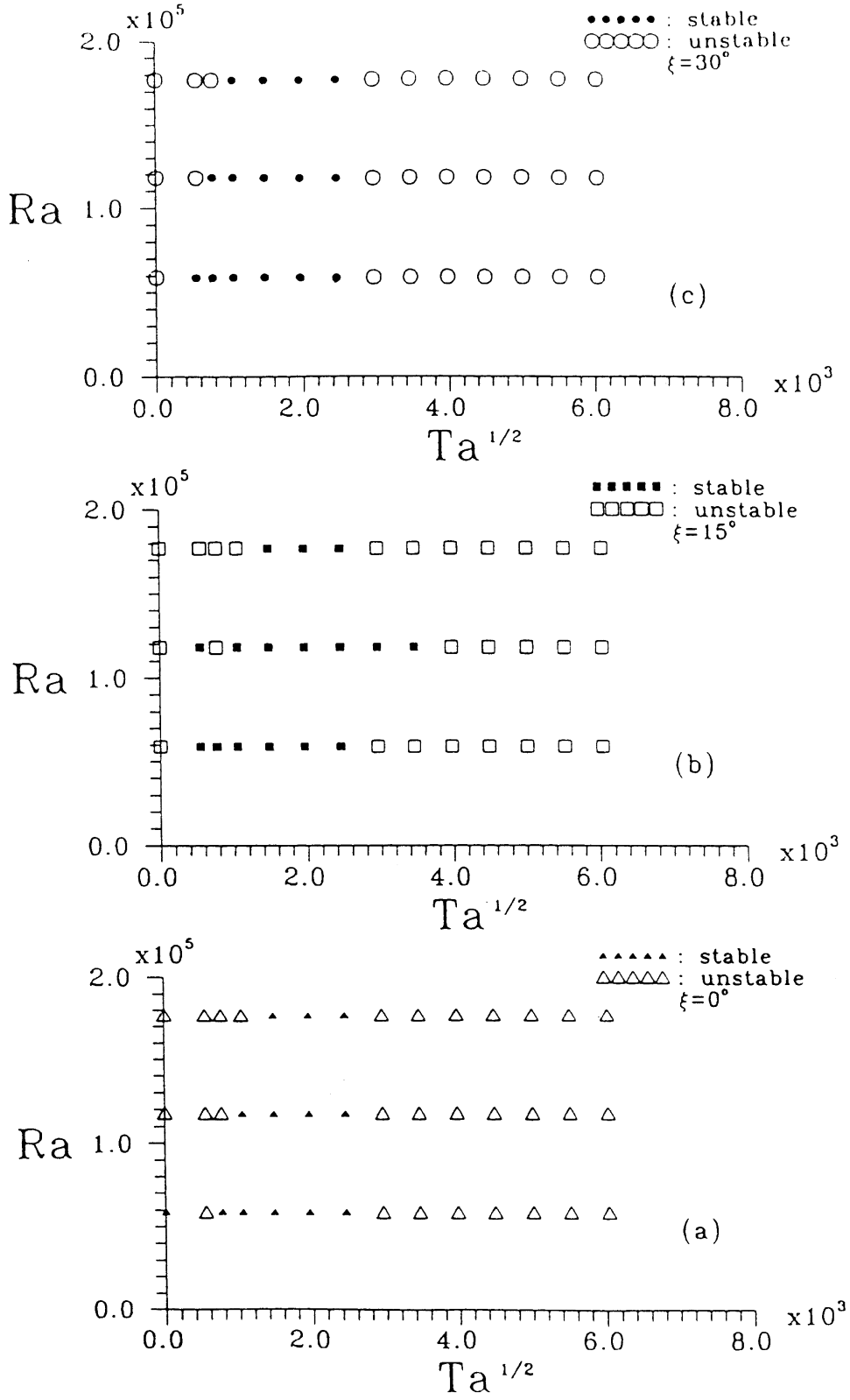

Fig. 11. Flow regime maps delineating the stable and unstable states of the oscillations for cylinder with diverging angle (a) $\xi = 0°$, (b) $\xi = 15°$ and (c) $\xi = 30°$.

flow oscillation is dominated mainly by a single fundamental frequency which varies nonmonotonically with the rotation rate. Flow regime maps delineating the stable and unstable states of the oscillations are provided in Fig. 11 for practical applications. Finally, it is natural to ask whether the above conclusion is still applicable to other fluids. This remains to be explored in the future.

Acknowledgements

The financial support of this study by the engineering division of National Science Council of Taiwan, Republic of China through the contract NSC 83–0401 E–009–009, is greatly appreciated.

References

[1] Hudson JL, Tang D, Abell S. Experiments on centrifugal driven thermal convection in a rotating cylinder. J Fluid Mech 1978;86:147–59.
[2] Tang D, Hudson JL. Experiments on a rotating fluid heated from below. Int J Heat Mass Transfer 1983;26:943–9.
[3] Chew JW. Computation of convective laminar flow in rotating cavities. J Fluid Mech 1985;153:339–60.
[4] Buell JC, Catton I. Effect of rotation on the stability of a bounded cylindrical layer of fluid heated from below. Phys Fluids 1983;26:892–6.
[5] Pfotenhauer JM, Niemela JJ, Donnelly RJ. Stability and heat transfer of rotating cryogens Part 3. Effects of finite cylindrical geometry and rotation on the onset of convection. J Fluid Mech 1987;175;85–96.
[6] Boubnov BM, Golitsyn GS. Experimental study of convective structures in rotating fluid. J Fluid Mech 1986;167:503–31.
[7] Kirdyashkin AG, Distanov VE. Hydrodynamics and heat transfer in a vertical cylinder exposed to periodically varying centrifugal forces (accelerated crucible rotation technique). Int J Heat Mass Transfer 1990;33:1397–415.
[8] Pulicani JP, Krukowski S, Iwan J, Alexander D, Ouazzani J, Rosenberger F. Convection in an asymmetrically heated cylinder. Int J Mass Transfer 1992;35:2119–30.
[9] Feigelson RS, Route RK. Vertical Bridgman growth of CdGeAs_2 with control of interface shape and orientation. Journal of Crystal Growth 1980;49:261–73.
[10] Dutta PS, Sangunni KS, Bhat HL, Kumar V. Growth of gallium antimonide by vertical Bridgman technique with planar crystal–melt interface. Journal of Crystal Growth 1994;141:44–50.
[11] Homsy GM, Hudson JL. Heat transfer in a rotating cylinder of fluid heated from above. Int J Heat Mass Transfer 1971;14:1149–659.
[12] Figliola RS. Convection transitions within a vertical cylinder heated from below. Phys Fluids 1986;29:2028–31.
[13] Olson JM, Rosenberger F. Convective instabilities in a closed vertical cylinder heated from below. Part 1. Monocomponent gases. J Fluid Mech 1978;92:609–29.
[14] Abernathey JR, Rosenberger F. Time-dependent convective instabilities in a closed vertical cylinder heated from below. J Fluid Mech 1985;160:137–54.
[15] Kamotani Y, Weng FB, Ostrach S. Oscillatory natural convection of a liquid metal in circular cylinders. Journal of Heat Transfer 1994;116:627–32.
[16] Niller PP, Bisshopp FE. On the influence of Coriolis force on onset of thermal convection. J Fluid Mech 1965;22:753–61.
[17] Veronis G. Large amplitude Bënard convection in a rotating fluid. J Fluid Mech 1968;31:113–39.
[18] Küppers G, Lortz D. Transition from laminar convection to thermal turbulence in a rotating fluid layer. J Fluid Mech 1969;35:609–20.
[19] Rossby HT. A study of Bënard convection with and without rotation. J Fluid Mech 1969;36:309–35.
[20] Hunter C, Riahi N. Nonlinear convection in a rotating fluid. J Fluid Mech 1975;72:433–54.
[21] Rudraiah N, Chandna OP. Effects of Coriolis force and nonuniform temperature gradient on the Rayleigh–Bënard convection. Can J Phys 1986;64:90–9.
[22] Clever RM, Busse FH. Nonlinear properties of convection rolls in a horizontal layer rotating about a vertical axis. J Fluid Mech 1979;94:609–27.
[23] Abell S, Hudson JL. An experimental study of centrifugally driven free convection in rectangular cavity. Int J Heat Mass Transfer 1975;18:1415–23.
[24] Hathaway DH, Somerville RCJ. Three-dimensional simulations of convection in layers with tilted rotation vectors. J Fluid Mech 1983;126:75–89.
[25] Bühler K, Oertel H. Thermal cellular convection in rotating rectangular boxes. J Fluid Mech 1982;114:261–82.
[26] Condie SA, Griffiths RW. Convection in rotating cavity: modeling ocean circulation. J Fluid Mech 1989;207:453–74.